JOURNAL OF GENERAL VIROLOGY

RESEARCH ARTICLE

Stevens *et al.*, *Journal of General Virology* 2019;100:568–582
DOI 10.1099/jgv.0.001240

MICROBIOLOGY SOCIETY

OPEN MICROBIOLOGY

A low-passage insect-cell isolate of bluetongue virus uses a macropinocytosis-like entry pathway to infect natural target cells derived from the bovine host

Lisa M. Stevens,[1,2]‡ Katy Moffat,[1] Lyndsay Cooke,[1,2] Kyriaki Nomikou,[1]§ Peter P. C. Mertens,[1]§ Terry Jackson[1,*]† and Karin E. Darpel[1,2,*]†

Abstract

Bluetongue virus (BTV) causes an economically important disease in domestic and wildlife ruminants and is transmitted by *Culicoides* biting midges. In ruminants, BTV has a wide cell tropism that includes endothelial cells of vascular and lymphatic vessels as important cell targets for virus replication, and several cell types of the immune system including monocytes, macrophages and dendritic cells. Thus, cell-entry represents a particular challenge for BTV as it infects many different cell types in widely diverse vertebrate and invertebrate hosts. Improved understanding of BTV cell-entry could lead to novel antiviral approaches that can block virus transmission from cell to cell between its invertebrate and vertebrate hosts. Here, we have investigated BTV cell-entry using endothelial cells derived from the natural bovine host (BFA cells) and purified whole virus particles of a low-passage, insect-cell isolate of a virulent strain of BTV-1. Our results show that the main entry pathway for infection of BFA cells is dependent on actin and dynamin, and shares certain characteristics with macropinocytosis. The ability to use a macropinocytosis-like entry route could explain the diverse cell tropism of BTV and contribute to the efficiency of transmission between vertebrate and invertebrate hosts.

INTRODUCTION

Arthropod-borne viruses (Arboviruses) are a diverse group of viruses that collectively cause a wide range of important diseases in man, domesticated animals and wildlife [1]. Arboviruses are transmitted between susceptible vertebrate hosts by arthropods, such as mosquitoes, ticks, fleas, sand flies and *Culicoides* spp. [2]. *Bluetongue virus* is the type species of the arbovirus genus *Orbivirus* (within the family *Reoviridae*). Bluetongue viruses (BTV) are transmitted by their biological vector, *Culicoides* biting midges, and can cause a severe hemorrhagic disease [bluetongue (BT)], particularly in naïve individuals belonging to certain species of domesticated and wild ruminants. Currently, at least 27 serotypes of BTV have been recognized with further additional serotypes proposed [3–7]. Historically, BTV was confined to tropical and temperate areas of Africa, America, Australia and Asia. However, in the last two decades BTV has greatly expanded its geographical distribution northwards culminating in 2006 in a BTV-8 strain spreading for the first time across Northern Europe, reaching as far as Scandinavia [8, 9], which has increased concerns over the potential for further significant BT outbreaks in the region.

The BTV virion comprises ten linear double-stranded RNA (dsRNA) segments encased within a three-layered capsid structure [10, 11]. The outer capsid is formed by VP2 and VP5, with the surface of the inner capsid (or 'core') formed by VP7. The innermost sub-core layer is

Received 31 October 2018; Accepted 12 February 2019; Published 7 March 2019
Author affiliations: [1]The Pirbright Institute, Ash Road, Pirbright, GU24 0NF, UK; [2]University of Surrey, Guildford, Surrey, GU2 7XH, UK.
***Correspondence:** Terry Jackson, terry.jackson@pirbright.ac.uk; Karin E. Darpel, karin.darpel@pirbright.ac.uk
Keywords: endocytosis; macropinocytosis; bluetongue virus; cell-entry; virus; bovine; endothelial cells.
Abbreviations: BTV, bluetongue virus; BFA, bovine foetal aorta endothelial; CME, clathrin mediated endocytosis; CPZ, chlorpromazine; CytoD, cytochalasin D; DAPI, 4'6-Diamidino-2-Phenylindole; DMSO, dimethylesulphoxide; DN, dominant negative; dsRNA, double stranded ribonucleic acid; Dyn2, dynamin 2; EIPA, 5-N-ethyl-N-isopropyl amiloride; FCS, flow cytometry standard; GFP, green fluorescent protein; GMEM, glasgow's minimum essential media; HCMV, human cytomegalovirus; ISVP, infectious sub-viral particles; MEVP, membrane enveloped virus particles; MFI, mean fluorescent intensity; MPC, micropinocytosis; NHE1, sodium proton exchanger 1; PBS, phosphate buffered saline; PFA, paraformaldehyde; PMA, phorbol-12- myristate-13-acetate; PAK1, p21-activated kinase 1; PI3K, phosphatidylinositol-3-kinase; RSV, respiratory syncytial virus; SSC, side scatter; WT, wild type.
†These authors contributed equally to this work.
‡Present address: Animal and Plant Health Agency, Woodham Lane, New Haw, KT15 3NB, UK.
§Present address: School of Veterinary Medicine and Science, University of Nottingham, Sutton Bonnington, Leicestershire, LE12 5RD, UK.
Three supplementary figures are available with this online version of this article.

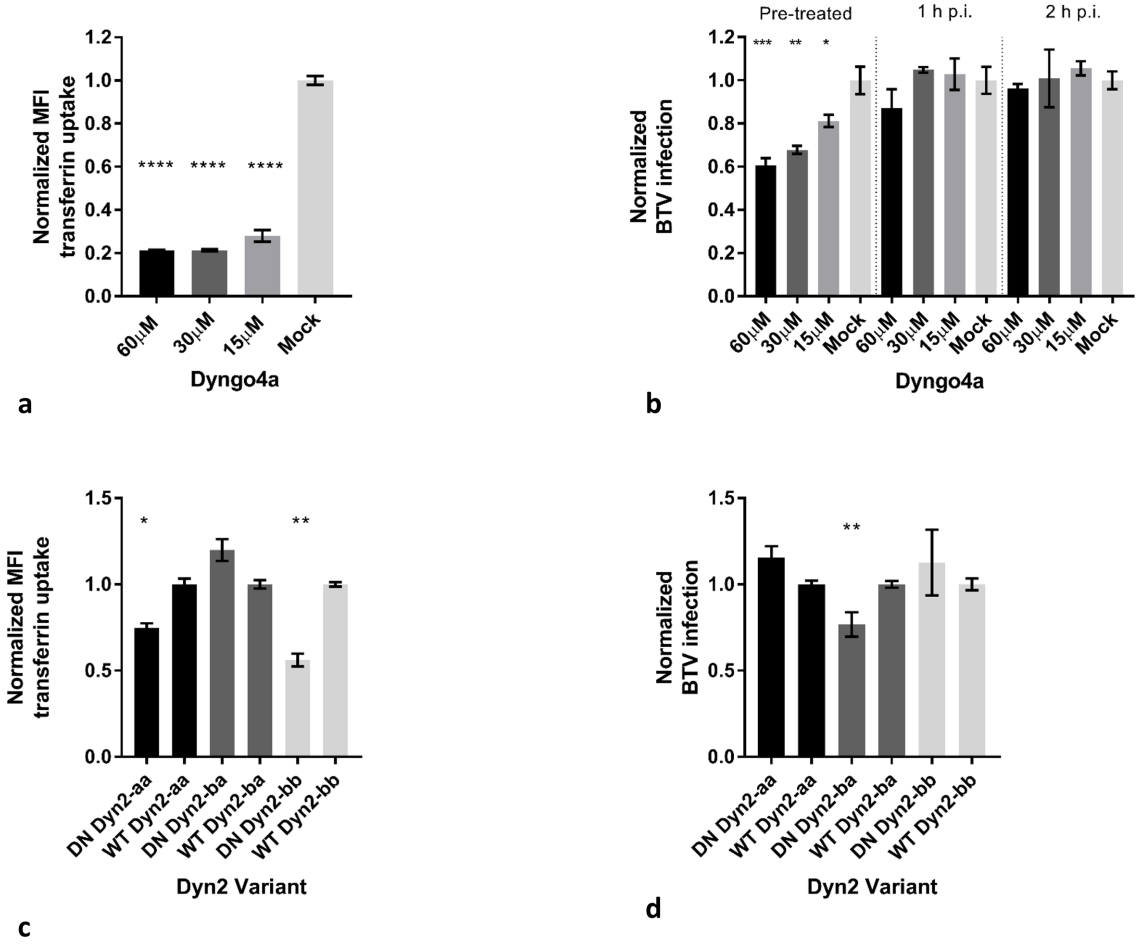

Fig. 1. BTV infection of BFA cells is partially inhibited by inhibitors of dynamin. Uptake of AlexaFluor-647-labelled transferrin (a) or BTV infection (b) of BFA cells treated with dyngo4a. Cells were mock-treated or treated with the drug at the indicated concentrations either as a pre-treatment or at the indicated times post-infection with BTV-1/KC3. In (b), the infection level for the control cells across the different mock-treatment time points was ~45 %. Transferrin uptake and infection were quantified by flow cytometry and the data normalized to the mock-treated cells. Data are shown as means+/-SEM for six technical replicates across two biologically independent experiments. BFA cells were transfected with the indicated DN Dyn2 splice variant (aa, ba or bb) or the matched WT protein as a GFP fusion protein prior to (c) AlexaFluor-647-labelled transferrin uptake or (d) infection with BTV-1/KC3. Transfection efficiencies (c and d) were between 83–89 % (WT/Dyn2 bb), 47–55 % (WT/Dyn2 ba) and 42–46 % (WT/Dyn2 aa). Infection levels for the GFP-positive cell populations expressing WT proteins was ~19 %. Transferrin uptake and infection were quantified by flow cytometry and the data normalized to the cells transfected with the matched WT Dyn2 construct. Data are shown as means+/-SEM for nine technical replicates across three biologically independent experiments *=*P*-value<0.05, **=*P*-value <0.005 and ***=*P*-value <0.0005.

composed of VP3 and surrounds the genomic dsRNA and the three protein components (VP1, VP4 and VP6) of the transcriptase complexes [11]. The outermost protein VP2, which represents the main target for neutralizing antibodies, determines BTV serotype specificity [12] and is the major cell-attachment protein [13–15], while VP5 is believed to play an active role in the penetration of cellular membranes during entry [13, 16, 17]. BTV whole virus particles are known to exploit receptor-mediated endocytosis to enter cells [17, 18]. On internalization, the low pH within acidic endosomes triggers VP2 dissociation and the fusion activity of VP5, ultimately delivering the complete core particle into the cytosol [17]. A number of endocytosis pathways have been recognized that deliver cargoes to acidic endosomes and of these, clathrin-mediated endocytosis (CME), caveolar/lipid raft-dependent endocytosis and macropinocytosis (MPC) have emerged as major cell-entry routes exploited by viruses [19]. These pathways may share some of the same molecular machinery; for example, dynamin is an important GTPase involved in endocytosis and serves as a scission factor during vesicle formation and plays a role in CME but also clathrin-independent endocytosis pathways including some types of MPC [20, 21].

The ability to enter cells determines viral cell- and tissue-tropism, and ultimately both host-range and disease manifestation. Cell-entry also represents a particular challenge for BTV

as it infects cells in widely diverse vertebrate and invertebrate hosts. Thus, enhancing our knowledge of cell-entry may help to develop antiviral reagents with the potential to block the initiation of BTV infections and their subsequent transmission. In its ruminant hosts, BTV infects a wide range of cell types, including several cells of the immune system such as monocytes, lymphocytes and conventional, follicular and plasmacytoid dendritic cells [22–25]. Endothelial cells of blood [25, 26] and lymphatic vessels [27] are also targeted by BTV and represent major sites of virus replication. Consequently, the most severe BT disease typically results in endothelial lesions, excessive bleeding and coagulopathy [25, 26, 28]. Despite its known cell tropism, it is not known if *in vivo* BTV utilizes conserved cell surface receptors and similar cell-entry mechanisms across different target cell types, or employs multiple entry strategies. In standard laboratory cell-lines, BTV has been reported to use more than one endocytosis pathway for cell-entry. Forzan *et al.* [17] reported that BTV-10 enters HeLa and Vero cells via CME [17], while we have shown that BTV-1 exploits a MPC-like entry pathway to infect BHK-21 cells [18]. The use of different entry pathways in these studies could be explained by the use of different BTV serotypes (which have significant variation in their cell attachment protein VP2), the use of alternative virus preparations (e.g. infectious tissue-culture supernatants or purified viral particles), or the use of different cell-lines that derive from species not normally targeted by BTV. However, although the above studies suggest BTV can use more than one entry pathway both used virus strains that had been passaged multiple times in tissue culture, thereby potentially adapting the virus to cultured cells. This could be significant as some viruses, such as foot-and-mouth disease virus and Japanese encephalitis virus, can acquire the ability to use alternative cell-attachment receptors (e.g. heparan sulphate) after cell culture adaptation, which could alter the entry route [29, 30]. With this in mind, recent studies [31] have demonstrated that a highly passaged strain of BTV-8 has an increased affinity for glycosaminoglycans; hence, serial cell passage could potentially modify the cell-entry characteristics of BTV field strains. Here, to provide further insight to BTV cell-entry, we have investigated the cell-entry pathway used by BTV-1 whole virus particles to infect natural target cells (endothelial cells) derived from the bovine host. For this study we a used a low-passage, purified virus that was isolated from a clinically ill sheep using an insect cell line [32]. Our results show that this strain preferentially uses a clathrin-independent, actin and dynamin dependent MPC-like pathway as the entry route to infect bovine endothelial cells.

RESULTS

BTV-1 infection of BFA cells is partially inhibited by inhibitors of dynamin but does not require clathrin-mediated endocytosis

To investigate cell-entry, we used a field-isolate of BTV-1 (BTV-1GIB2007) and a bovine foetal aorta endothelial cell line (BFA cells), representing one of the major cell-types targeted by BTV in the mammalian host. BTV-1 GIB2007/01 was originally isolated from infected sheep blood during a BT outbreak in Gibraltar in 2007 by a single passage in KC cells. This virus (from here on known as BTV-1/KC3) was subjected to two subsequent passages and virus particle purification using KC cells. The quality of the purified virus preparation was confirmed by silver stained SDS-PAGE (Fig. S1, available in the online version of this article) and virus infectivity was determined by titrating virus on BFA cells. Sequence analysis of genome segments 2, 3, 6 and 7 of BTV- 1/KC3, which encode the major structural proteins of the virus capsid VP2, VP3, VP5 and VP7 respectively, showed an identical consensus amino acid sequence to that of BTV-1GIB2007 at KC cell passage level 2 (KC2; isolate BTV-1GIB2007/06) (accession no.: KP821004, KP821126, KP821366, KP821608), suggesting that an additional passage in KC cells is unlikely to have induced cell culture adaptations that could affect the cell-entry pathway. In support of this conclusion, low-passage KC cell, BTV isolates have previously been shown to retain infectivity in experimental animal infection studies, which suggest they have not acquired mutations that alter cell-entry or virulence [33].

Previously, we reported that entry into BHK-21 cells by a highly passaged tissue-culture BTV-1 reference strain is most likely dynamin-dependent as entry was inhibited by dynasore, a commonly used inhibitor of dynamin [18]. However, we could not determine the effect of dynasore on infection due to a delayed cell toxicity [18]. Paradoxically, the same study showed that expression of a dominant-negative (DN) mutant of dynamin-2 (Dyn-2) had no effect on cell-entry or infection [18], suggesting that BTV entry may be dynamin-independent. Using BFA cells, our initial experiments showed that, similarly to our previous observations for BHK-21 cells [18], extended use of dynasore (at 100 μM) was toxic (data not shown). In contrast, dyngo4a (a less toxic derivative of dynasore that also inhibits dynamin) [34] was non-toxic up to 240 μM (Fig. S2). Dynamin is essential for clathrin-mediated endocytosis (CME), and consistent with this, Fig. 1(a) shows that dyngo4a (15-60μM) inhibited transferrin uptake (a commonly used ligand for CME) by BFA cells. Dyngo4a also inhibited BTV infection in a dose-dependent manner (Fig. 1b), but only when added as a pre-treatment and not when added at later times [1 and 2 h post-infection (h p.i.)] suggesting that BTV entry was dynamin-dependent. However, at the concentrations used, dyngo4a only had a partial inhibitory effect on BTV infection.

Mammalian dynamin is expressed as three isoforms (Dyn1, Dyn2 and Dyn3), and of these, Dyn2 is ubiquitously expressed [35]. Furthermore, Dyn2 exists as four splice variants ('aa', 'ab', 'ba' and 'bb') [36]. Our previous observation that BTV-1 infection of BHK-21 cells was not inhibited by a DN mutant of dynamin was made using the 'aa' splice variant [18]. To further investigate the role of dynamin in BTV infection, we transfected BFA cells to express DN mutants of three Dyn2 splice variants (DN-

Dyn2-aa, DN-Dyn2-bb and DN-Dyn2-ba) and quantified the effect on transferrin uptake (Fig. 1c) and BTV infection (Fig. 1d). Cells were transfected with the above DN mutants or with the corresponding matched WT Dyn2 splice variants as green fluorescent protein (GFP) fusion proteins. At 16 h post-transfection, the cells were incubated with transferrin or infected with BTV-1/KC3. Consistent with the role of dynamin in CME, over expression of DN-Dyn2-aa or DN-Dyn2-bb inhibited transferrin uptake (Fig. 1c); however, these mutants had no effect on BTV infection (Fig. 1d). In contrast, expression of DN-Dyn2-ba appeared to increase transferrin uptake, although this was not statistically significant (Fig. 1c) and partially inhibited BTV infection (Fig. 1d). These results are consistent with our previous observations using BHK-21 cells and a DN mutant of the Dyn-2 'aa' splice variant [18], and further, show that BTV infection is selectively inhibited by expression of a Dyn2 DN mutant of the 'ba' splice variant. Taken together, the above observations show that inhibition of dynamin results in a partial inhibition of infection and suggest that BTV may be able to infect BFA cells using more than one uptake pathway that differ in their dependency of dynamin (see Discussion).

The above results suggest that BTV entry into BFA cells is partially dynamin-dependent. In addition, the observations that DN Dyn2 mutants of the 'aa' and 'bb' splice variants inhibited transferrin uptake, but not BTV infection, are consistent with virus entry not occurring by CME. To further investigate BTV entry, BFA cells were incubated with Alexa-Fluor 568-labelled transferrin (which is taken up by CME [37]) or with BTV-1/KC3 for 15 min at 37 °C and the cells processed for confocal microscopy labelling for BTV-1 capsid proteins. In these experiments, the actin cortex was also labelled using Cytopainter 405-labelled phalloidin or Alexa-Fluor-647 phalloidin, respectively, to judge if transferrin or virus was at the cell surface or internalized (i.e. located outside or underneath the actin cortex). Fig. 2 shows extensive transferrin uptake by BFA cells after 15 min (Fig. 2a), while BTV particles were not present within the cytosol and remained at the cell surfaces (Fig. 2b, c). This experiment shows that BTV is internalized at a slower rate than transferrin and adds support to the conclusion that despite its partial dynamin requirement, BTV entry does not occur via CME but instead relies on a clathrin-independent pathway.

To confirm if dyngo4a blocked BTV entry, mock and dyngo4a-treated cells were infected with BTV-1/KC3 for 2 h and processed for confocal microscopy labelling for BTV-1 capsid proteins and actin. Using fields of view through the central Z-stacks, 22 BTV-positive mock-treated cells were randomly selected and all showed viral capsid labelling within the cytosol (average 13 BTV puncta/cell) in addition to virus at the cell surface (average eight BTV puncta/cell). Fig. 2(d) shows a typical mock-treated cell and labelling for BTV capsid proteins inside and outside the cytosol (note, for some images in Fig. 2 actin labeling is not shown for clarity). In contrast, central Z-stacks of dyngo4a-treated cells showed that, in addition to BTV present on the cell surfaces, only 22 of 40 BTV-positive cells had some BTV puncta in the cytosol (average 1.5 BTV puncta/cell) while BTV capsid labelling for the other 18 cells was completely confined to the cell surfaces. Fig. 2 (e, f) show dyngo4a treated cells, and for some, BTV labelling was confined to the cell surface (Fig. 2e) while for others a small amount of virus labelling was also present within the cytosol (arrowed in Fig. 2f). Although not providing an exact quantification of BTV uptake (as we used central Z-stacks), the above observations suggest that the majority of BTV uptake is inhibited by dyngo4a and therefore dynamin-dependent. These results are consistent with the incomplete inhibitory effect of dyngo4a on BTV infection (Fig. 1b) and suggest that dynamin is most likely required for the preferred cell-entry pathway used by BTV. However, the incomplete block to virus entry caused by dyngo4a suggests that virus uptake could also be occurring via an alternative, dynamin-independent endocytosis pathway (see Discussion).

To further confirm that CME was not required for BTV infection, BFA cells were treated with pitstop-2 or chlorpromazine (CPZ), drugs that inhibit CME by preventing assembly of clathrin-coated pits [38, 39]. Initial experiments confirmed that pitstop-2 (up to 200 μM) and CPZ (up to 10 μg ml^{-1}) were non-toxic for BFA cells (Fig. S2). Fig. 3(a) shows that pitstop-2 (25 μM), but not CPZ (10 μg ml^{-1}) inhibited transferrin uptake, indicating that in BFA cells, CME was blocked only by pitstop-2. Higher concentrations of CPZ showed toxicity for BFA cells (Fig. S2), restricting its further use to investigate its effect on BTV infection. Despite inhibiting transferrin uptake, pitstop-2 did not significantly inhibit BTV infection by BTV-1/KC3 (Fig. 3b) thereby supporting the conclusion that the main entry pathway for BTV into BFA cells is independent of CME. We also evaluated the role of CME in BTV-1/KC3 infection of BFA cells using DN mutants (DIII and EH29) of eps15 (a clathrin cage recruitment factor), which are known to inhibit CME [40, 41]. Both mutants inhibited transferrin uptake when compared to cells transfected to express a control eps15 construct (D3Δ2) that does not interfere with CME (Fig. 3c). In contrast, expression of the mutant constructs did not significantly inhibit BTV infection (Fig. 3d). Together, the above results show that although dynamin inhibitors reduced BTV-1/KC3 cell-entry and infection, infection does not require CME and suggest that a clathrin-independent endocytosis pathway serves as the major route used for BTV entry into BFA cells.

BTV-1 delivery to acidic compartments

Infection by whole BTV particles is dependent on virus acidification [17, 18]. To gain further insight into BTV cell-entry kinetics, we determined the time taken for virus to be delivered to acidic compartments using ammonium chloride, which increases the pH within the endosomal-lysosomal system and thereby prevents BTV acidification and infection. BFA cells were mock-treated or incubated with ammonium chloride, either as a pre-treatment or at different times after infection, and the drug then remained

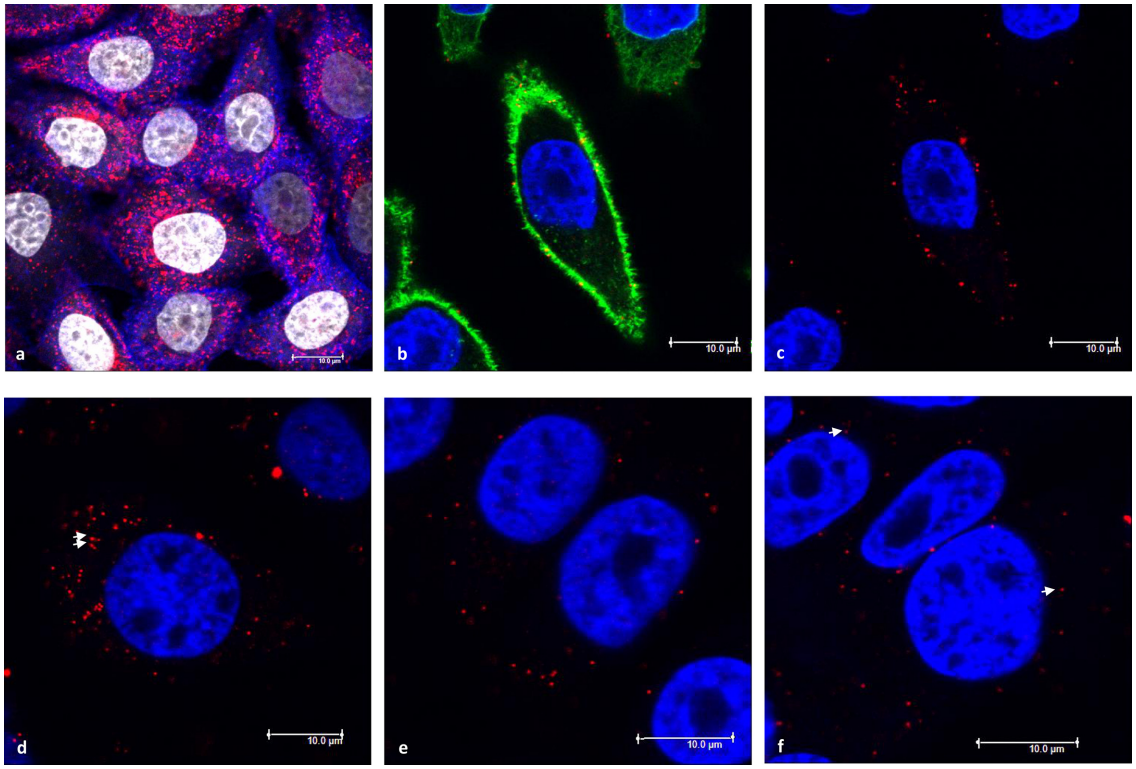

Fig. 2. BTV cell-entry follows different kinetics to transferrin uptake. (a) Uptake of AlexaFluor-647-labelled transferrin (red) by BFA cells after 15 min at 37 °C. The actin cortex was labelled with CytoPainter-405 labelled phalloidin (blue) and the cell nuclei labelled with TO-PRO-3 (white). (b) Uptake of BTV-1/KC3 (MOI=10) (red) by BFA cells after 15 min at 37 °C. The actin cortex was labelled with AlexaFluor-488-labelled phalloidin (green) and the cell nuclei labelled with DAPI (blue). (c) The same cell as in (b) without actin labelling. (d) Uptake of BTV-1/KC3 (m.o.i.=10) (red) by mock-treated BFA cells after 2 h at 37 °C. (e and f) BTV uptake by BFA cells for 2 h in the presence of dyngo4a (30 µM). Surface and internalized virus were judged by the position relative to the actin cortex. For clarity actin labelling is not shown. Arrows on (d and f) indicate internalized virus. BTV capsid proteins were labelled using ORAB276. Scale bar, 10 µm.

present throughout the rest of the assay. After 16 h, infection was stopped by the addition of PFA and the level of infection quantified by flow cytometry and normalized to the mock-treated cells. As expected, a strong inhibitory effect was seen when ammonium chloride was added as a pre-treatment (Fig. 4). Infection was also significantly inhibited when the drug was added at 1 h p.i. When added at later times, infection was also inhibited, albeit to non-significant levels (Fig. 4). These results suggest that BTV-1/KC3 is delivered to acid compartments at a slower rate than expected for CME (see also Fig. 2) and add support to the conclusion that CME is not the major entry pathway [42, 43] used to infect BFA cells.

BTV-1 infection of BFA cells is dependent on actin dynamics and macropinocytosis

The actin cortex reinforces the plasma membrane and is dynamically regulated during the formation of endocytic vesicles [44] and some viruses disrupt actin to facilitate uptake [45]. Therefore, we investigated the effect of BTV on actin during the early phase of infection (Fig. 5). BTV-1/KC3 was pre-bound to BFA cells at 4 °C for 1 h before warming to 37 °C to initiate entry. At the indicated times post-warming, the cells were fixed and processed for confocal microscopy labelling for BTV-1 capsid proteins and actin using AlexaFluor-488-labelled phalloidin. At 0 h (i.e. before warming), virtually all virus labelling appeared to be outside of the actin cortex while some virus appeared to be in close association with actin filaments that projected away from the cells (Figs 5a, b and S3). At 0.5 h post-warming, virus labelling was still not evident within the cytosol and virtually all remained at the cell periphery, i.e. outside of the actin cortex (Figs 5c, d and S3). At these time points, all cells (BTV-positive and BTV-negative) appeared to have an intact actin cortex (Figs 5a and 5c). Similarly, the actin cortex appeared intact for virtually all (>95 %) of the BTV-negative cells at 1 and 1.5 h post-warming. By 1.5 h post-warming, virus capsid labelling was clearly evident within the cytosol (Figs 5g, h and S3). However, in contrast to the BTV negative cells, at 1 and 1.5 h post-warming the majority of BTV-positive cells showed a markedly different pattern for actin (Fig. 5e, g and S3) and the actin cortex

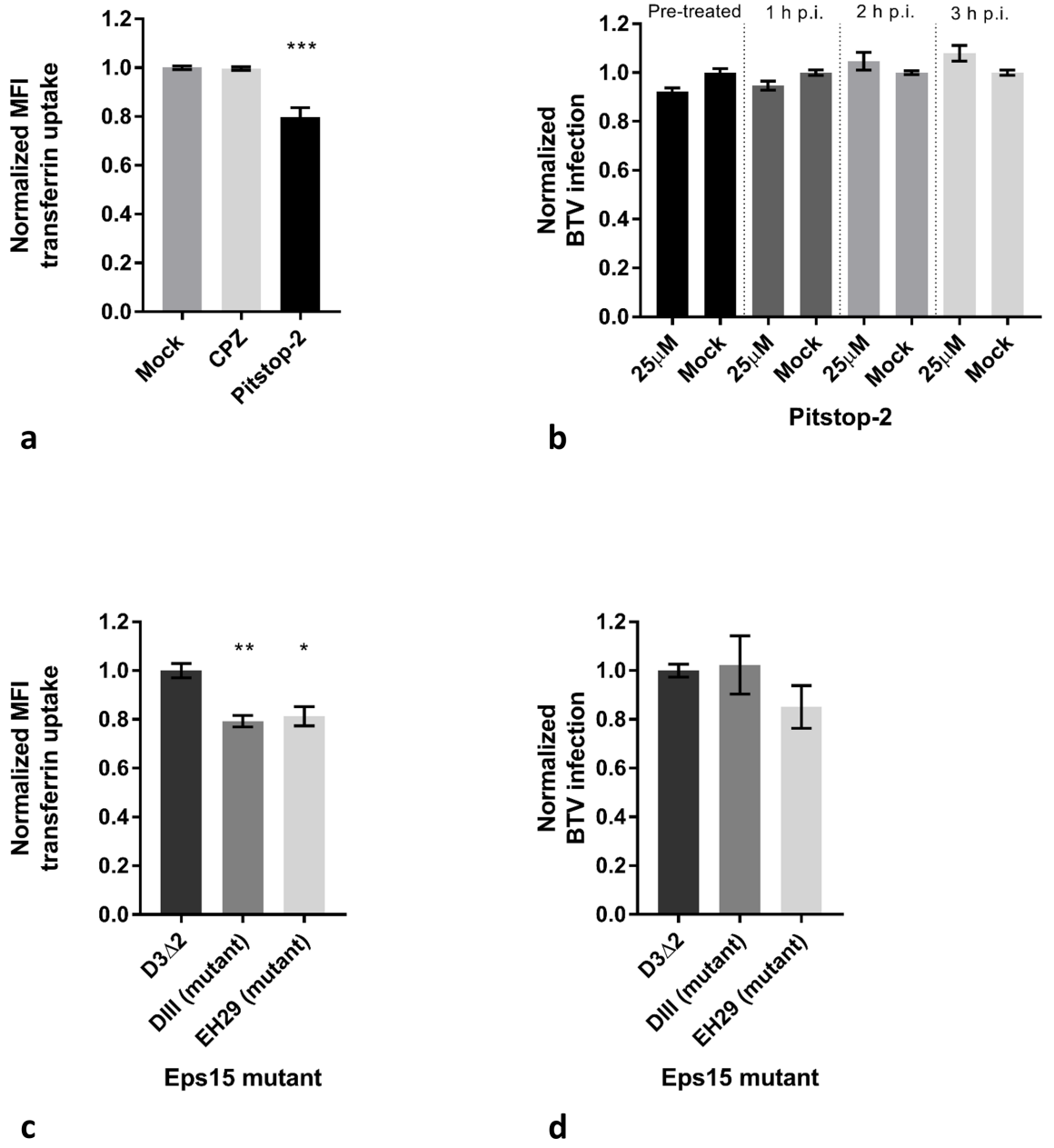

Fig. 3. BTV infection of BFA cells is clathrin-independent. (a) Uptake of AlexaFluor-647-labelled transferrin by BFA cells pre-treated with clathrin inhibitors [10 μg ml^{-1} chlorpromazine (CPZ) or 25 μM pitstop-2]. (b) The effect of pitstop-2 on infection of BFA cells. Cells were mock-treated or treated with pitstop-2 (25 μM) either as a pre-treatment or at the indicated times post-infection with BTV-1/KC3. The infection level for the control cells across the different mock-treatment time points was ~50 %. Transferrin uptake and infection were quantified by flow cytometry and the data normalized to the mock-treated cells. BFA cells were transfected with the indicated DN eps15 construct (DIII or EH29) or the D3Δ2 control as a GFP fusion protein prior to (c) AlexaFluor-647-labelled transferrin uptake or (d) infection with BTV-1/KC3. Transferrin uptake and infection were quantified by flow cytometry and the data normalized to the cells transfected with the D3Δ2 control. Transfection efficiencies (c and d) were between 30 and 45 %. Infection levels for the GFP-positive cell populations expressing D3Δ2 was ~25 %. For each experiment, data are shown as means+/-SEM for six technical replicates across two biologically independent experiments. *=*P*-value<0.05, **=*P*-value<0.005 and ***=*P*-value<0.0005.

appeared to be disrupted. Fig. 5(g) shows a side-by-side comparison of typical actin labelling for BTV-positive and BTV-negative cells. Quantification of the effect of BTV on the actin cortex is shown in Fig. 5(i, j). The actin cortex was observed using central Z-stacks through the cells across randomly selected fields of view. At 1 h post-warming only

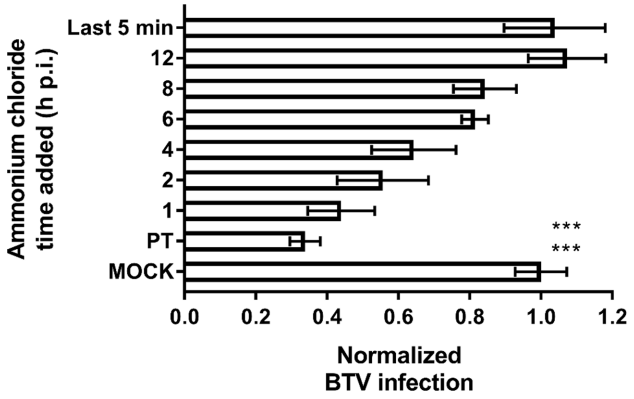

Fig. 4. BTV delivery kinetics to acidic compartments. BFA cells were mock-treated or treated with ammonium chloride (25 mM) as a pre-treatment or at the indicated times post infection with BTV-1/KC3. Infection level of the mock-treated cells was ~60 %. The number of infected cells was quantified by flow cytometry and normalized to the level of infection of the mock-treated cells. Data are shown as means+/-SEM for six technical replicates across two biologically independent experiments ***=*P*-value<0.0005.

~16 % (*n*=34 cells) of the BTV-positive cells had an intact cortex while for ~84 % (*n*=184 cells) the cortex appeared disrupted. Similar results were observed at 1.5 h post-warming as ~76 % (*n*=222 cells) of the BTV-positive cells showed a disrupted actin cortex. However, the disruption appeared to be transient as at 2 h post-warming the actin cortex appeared to be reforming for some of the BTV-positive cells (Fig. S3). These observations show that that cell-entry coincides with disruption of the actin cortex and suggest that actin rearrangements may be important for BTV internalization.

To test if actin is important for infection we used cytochalasin D (cytoD), which inhibits actin polymerization. Our initial experiments showed that cytoD was non-toxic for BFA cells up to 160 μg ml^{-1} (Fig. S2) and at 10 μg ml^{-1}, caused a major rearrangement of actin (Fig. 6a-d). In addition, when added as a pre-treatment, or at 1 or 2 h p.i., cytoD inhibited BTV-1/KC3 infection of BFA cells. In contrast, an inhibitory effect was not seen when the drug was added at 3 h p.i. (Fig. 6e). Thus, inhibition of BTV infection by cytoD occurred with similar kinetics to virus internalization (Fig. 5) and delivery to acidic endosomes (Fig. 4), suggesting that actin dynamics plays an important role in the infection process.

Macropinocytosis (MPC) is an actin-dependent process [46] and results in increased fluid-phase uptake. In some cell types (e.g. professional phagocytes) MPC is constitutively active, while in others it requires activation [44, 47]. Some viruses activate MPC for cell-entry [44]; thus, infection by such viruses can be accompanied by elevated fluid-phase uptake [48, 49]. Phorbol esters, such as phorbol-12-myristate-13-acetate (PMA) also induce MPC and increase fluid-phase uptake. To determine if BTV induces fluid-phase uptake, BFA cells were incubated with BTV-1/KC3 (m.o.i.=5) or PMA (1 μg ml^{-1}) for 15 min before adding AlexaFluor-647-labelled dextran (0.5 mg ml^{-1}), a marker of fluid-phase uptake [50]. After a further 15 min, the cells were fixed and dextran uptake quantified by flow cytometry. Both PMA and BTV stimulated dextran uptake compared to mock-treated cells, and to a comparable extent, suggesting that BTV may also stimulate fluid-phase uptake, possibly by MPC (Fig. 7a).

MPC is dependent on sodium/proton exchangers (NHE) [51, 52] and inhibited by EIPA (5-(N-ethyl- N-isopropyl) amiloride), which targets NHE1 (55). PAK-1 is also required for MPC [50–52] and inhibition of PAK-1 by IPA3 (56) also inhibits MPC [44]. Thus, EIPA and IPA3 are often used as inhibitors of MPC [44, 53, 54] (see Discussion). In some cell types, MPC is also dependent on cellular kinases, including phosphatidylinositol-3-kinase (PI3K) [55]; thus, inhibition of PI3K by wortmannin may also inhibit MPC [56]. Our initial experiments established that EIPA (up to 200 μM), IPA3 (up to 200 μM) and wortmannin (up to 800 nM) were non-toxic for BFA cells (Fig. S2). Fig. 7(b) shows that IPA3, but not EIPA inhibited dextran uptake suggesting that, for BFA cells, IPA3 may be a more potent inhibitor of MPC/fluid-phase uptake. However, when added either as a pre-treatment or up to 3 h p.i. both EIPA (Fig. 7c) and IPA3 (Fig. 7d) had strong inhibitory effect on BTV infection. In contrast, neither drug had a significant effect on BTV infection when added at 6 h p.i. (data not shown). The same experiments were carried out using wortmannin but we did not see an inhibitory effect on either dextran uptake (Fig. 7b) or BTV infection (data not shown). These results suggest that BTV-1/KC3 may utilize MPC or a MPC-like pathway for infection of BFA cells. However, since neither dextran uptake nor BTV infection was inhibited by wortmannin, BTV entry into BFA cells may not require PI3K (see Discussion).

DISCUSSION

Here we have shown that a low-passage insect-cell isolate of a virulent BTV-1 field strain (BTV-1/KC3) preferentially utilizes an actin- and dynamin-dependent MPC-like

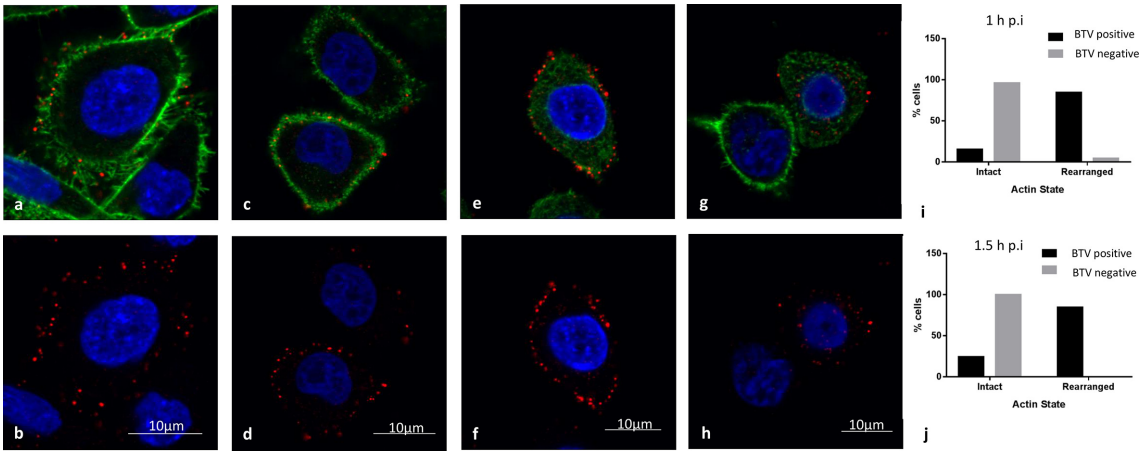

Fig. 5. BTV entry coincides with disruption of the actin cortex. BFA cells were incubated with BTV-1/KC3 (m.o.i=10) at 4 °C before infection at 37 °C. Infection was stopped at 0 (a and b), 0.5 h p.i. (c and d), 1 h p.i. (e and f) or at 1.5 h p.i. (g and h). BTV capsid proteins are shown in red, the cell nuclei in blue and the actin cortex in green (scale bar, 10 µm). (b, d, f and h) show the same cells as in (a, c, e and g) but with the actin labelling removed. Quantification of actin cortex disruption for BTV-positive and BTV-negative cells at 1 h p.i. (i) and 1.5 h p.i. (j) Data are shown as representative for 12 technical replicates across 4 biologically independent experiments.

endocytosis pathway to infect endothelial cells derived from the natural bovine host. This conclusion is based on the observations that; (i) BTV-1/KC3 triggered a major disruption of the actin cortex during entry and elevated fluid-phase uptake during the early phase of infection, (ii) infection was inhibited by actin disruption, and (iii) by known MPC inhibitors (EIPA and IPA3). Furthermore, we found no evidence for the involvement of CME in BTV infection as entry followed different kinetics to transferrin uptake and established pharmacological and DN inhibitors of CME did not appear to inhibit infection. Thus, our study shows that BTV joins a growing number of diverse viruses that can enter mammalian cells via MPC or MPC-like endocytosis pathways [44, 57–61]. However, it should be noted that in addition to whole virus particles, BTV can exist as at least three other infectious particle types including temporarily membrane enveloped virus particles (MEVP), infectious sub-viral particles (ISVP) and core particles. These different particle types have different specific infectivity for mammalian and insect cells [62] and different outermost surface-components that are likely involved in cell attachment and could potentially influence the cell-entry route. Therefore, it is important to state that our results may only be relevant for whole virus particles and further work will be required to determine the cell-entry route used by other BTV particle types.

EIPA and IPA3 are commonly used to investigate if viruses enter cells by MPC or MPC-like routes. Viruses reported to use MPC as their major cell-entry route include measles [61], influenza [58], respiratory syncytial virus (RSV) [60], and human cytomegalovirus (HCMV) [59] and in these studies treatment with EIPA or IPA3 reduced respective viral infection by about 65–70 %. Here we have shown that BTV infection is inhibited to a similar extent following treatment with either EIPA or IPA3. Our results with EIPA and IPA3 are consistent with inhibition of cell-entry, as the effects on infection were maximal when they were added during the early phase of infection (Fig. 7) and they did not significantly affect BTV infection when added at later times. Furthermore, the inhibitory effects of EIPA and IPA3 of BTV infection followed similar kinetics to inhibition by cytoD (which would inhibit actin remodelling during MPC), and with the rate of BTV delivery to acidic compartments, supporting the notion that the reduction of BTV infection by these reagents is achieved via inhibition of MPC. Nonetheless, while some studies report that EIPA selectively inhibits MPC with little or no effect on other endocytosis pathways [51], some investigations have reported that EIPA might also inhibit cellular processes such as actin remodelling, internalization of lipid rafts and CME [63–66]. EIPA has also been shown to have an indirect effect on adenovirus infection by preventing virus-induced MPC and thereby reducing virus escape from endosomes following virus uptake by CME [67]. Additionally, actin depolymerization drugs (such as CytoD) do not solely inhibit MPC, as actin is required for different types of endocytosis [68]. Thus, although we cannot completely exclude that the effects of the inhibitors used in our study on BTV infection may not result solely from effects specific to MPC, we found no evidence that BTV infects BFA cells via CME, as infection was not significantly inhibited by pitsop-2, or expression of DN inhibitors of CME that were shown to inhibit CME of transferrin (Fig. 3).

Several studies have shown that dynamin is not usually required for MPC [69]. However, dynamin has been

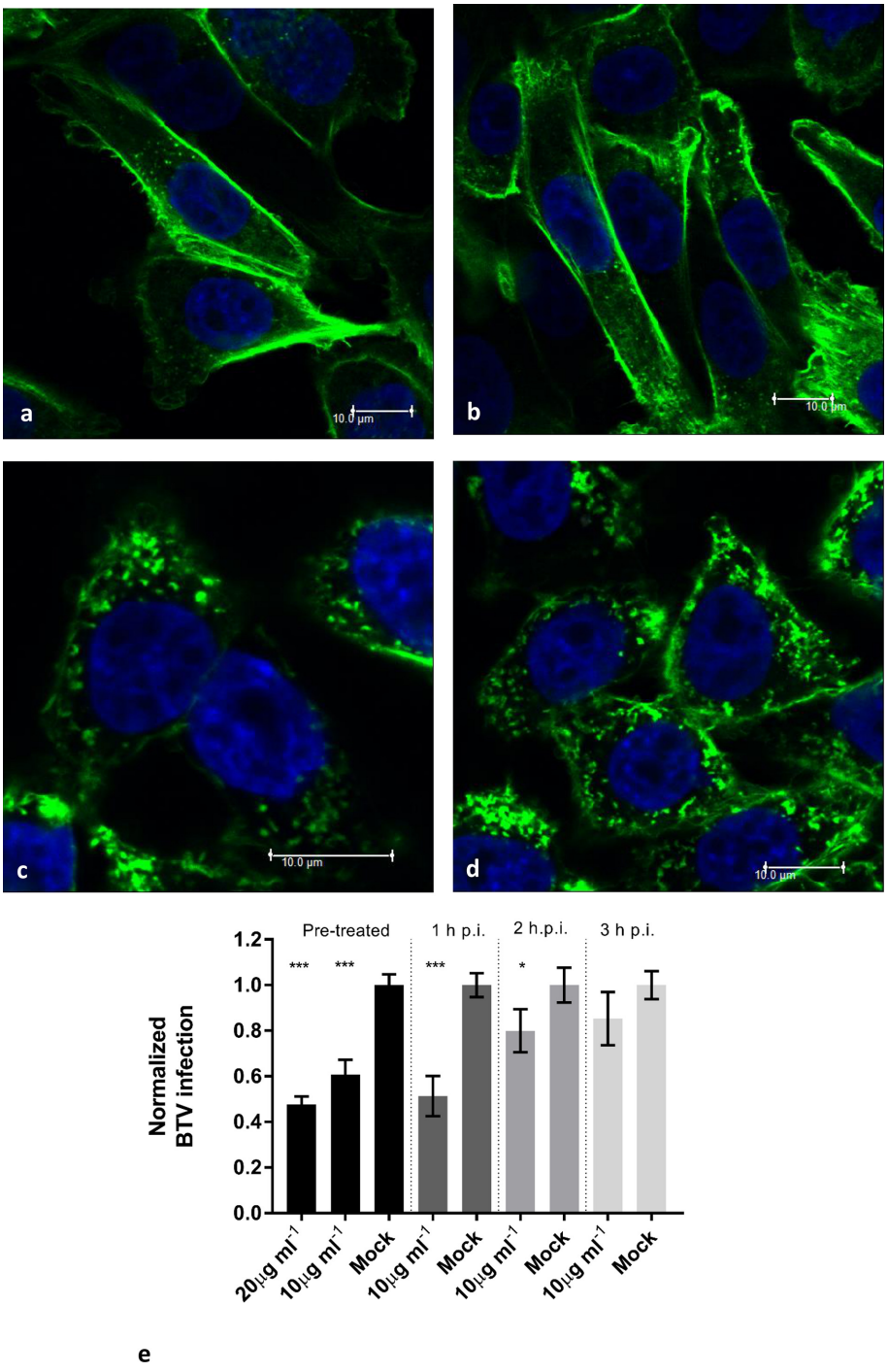

Fig. 6. BTV infection of BFA cells is inhibited by actin disruption. BFA cells were mock-treated (a) and (b) or pre-treated with cytochalasin D (10 µg ml^{-1}) (c) and (d) prior to actin labelling using AlexaFluor-488-labelled phalloidin (green). The cell nuclei are shown in blue. Scale bar, 10 or 20 µm. BFA cells were mock-treated, or treated with cytochalasin D at the indicated concentrations either as a pre-treatment or at the indicated times post-infection (h p.i.) with BTV-1/KC3. Infection level for the control cells across the different mock-treatment time points was ~31 %. Infection was quantified by flow cytometry and the data normalized to the mock-treated cells. Data are shown as means+/-SEM for six technical replicates across two biologically independent experiments. *=*P*-value<0.05, ***=*P*-value<0.0005.

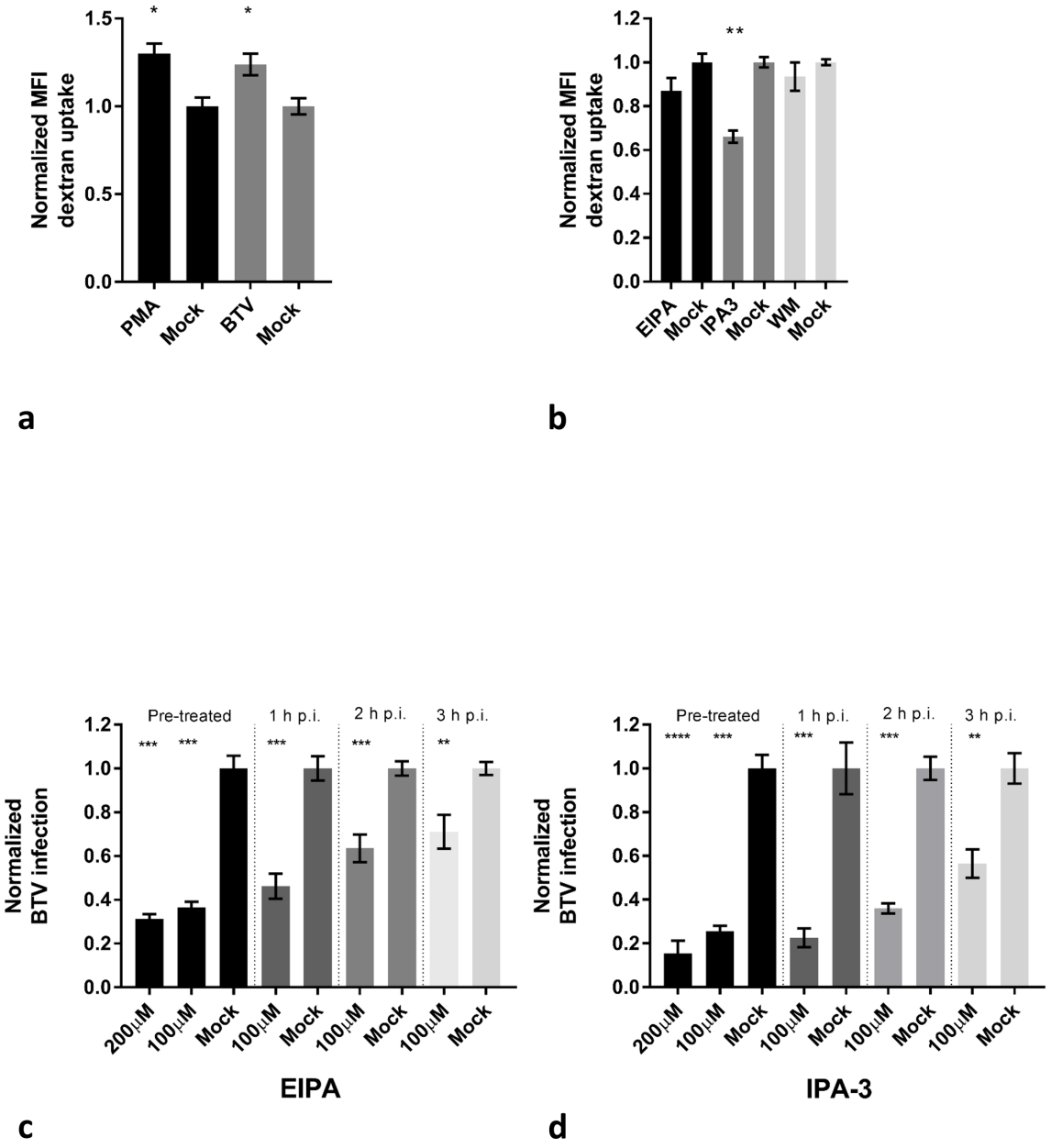

Fig. 7. BTV infection of BFA cells shows characteristics of MPC. BFA cells were mock-treated, or treated with PMA (1 μg ml^{-1}) or BTV (m.o.i.=5) for 15 min prior to the addition of AlexaFluor-647-labelled dextran (0.5 mg ml^{-1}) for 15 min (a). Dextran uptake was quantified by flow cytometry and the data normalized to the mock-treated cells. (b) BFA cells were mock-treated, or treated with EIPA (100 μM), IPA3 (100 μM) or wortmannin (WM) (200 nm) for 0.5 h prior to the addition of AlexaFluor-647-labelled dextran (0.5 mg ml^{-1}) for 15 min. Dextran uptake was quantified by flow cytometry and the data normalized to the mock-treated cells. BFA cells were mock-treated, or treated with (c) EIPA (100 μM) or (d) IPA3 (100 μM) either as a pre-treatment or at the indicated times post-infection with BTV-1/KC3. Infection level for the control cells across the different mock-treatment time points were ~33 % (c) and ~32 % (d). Infection was quantified by flow cytometry and the data normalized to the mock-treated cells. For each experiment, data are shown as means+/-SEM for six technical replicates across two biologically independent experiments. *=*P*-value<0.05, **=*P*-value<0.005 and ***=*P*-value<0.0005.

implicated in the regulation of actin dynamics [70] and some types of non-canonical MPC have been shown to be dynamin-dependent [58, 71, 72]. Thus, despite sharing some characteristics of MPC, our results show the main entry route used by BTV to infect BFA cells appears to deviate from canonical MPC, as entry was dynamin-dependent. Consistent with the existence of dynamin-independent and dynamin-dependent MPC pathways [69], infection by other viruses that use MPC for entry have been reported to have different requirements for dynamin [57–61, 71, 73].

For example, cell-entry by measles, influenza, RSV and vaccinia virus does not require dynamin, whereas entry of HCMV is dynamin-dependent [59]. Thus, similar to HMCV our results show that infection by BTV is mediated by a MPC-like pathway that is dynamin-dependent; however, for HCMV dyngo4a (25 μM) inhibited infection by a greater extent (>90 %) than we observed for BTV with BFA cells (~35 % inhibition with dyngo4a 30 μM). Thus, due to the incomplete inhibition of entry and infection caused by dyngo4a our results could be interpreted to show that BTV may be able to enter BFA cells by more than one pathway that differ in their dependency on dynamin. Further investigations will be needed to determine if this is the case and if this involves a pathway distinct to MPC or two alternative MPC-like pathways that differ in their dependency on dynamin. Nevertheless, the inability to inhibit BTV infection of BFA cells using reagents that reduce CME suggest that if a second dynamin-dependent endocytosis process mediates BTV internalization then this pathway would most likely be independent of clathrin.

Consistent with the partial inhibitory effect on infection seen for dyngo4a, infection of BFA cells was also inhibited by expression of a DN mutant of dynamin-2. Interestingly, our results also show that a DN mutant of Dyn2 'ba' splice variant (DN-Dyn2-ba) preferentially inhibited BTV infection. In support of this conclusion, expression of DN-Dyn2 mutants of the 'aa' and 'bb' splice variants inhibited transferrin uptake but did not appear to inhibit infection, whereas DN-Dyn2-ba did not inhibit transferrin uptake but did inhibit BTV infection. These results suggested that, in BFA cells, the different Dyn2 splice variants may have distinct roles in endocytosis. This conclusion is supported by studies that show that the dynamin-2 splice variants have different functions, including distinct roles in endocytosis [36, 74], and are consistent with a study that showed that the 'ba' splice variant of Dyn2 is required for PDGD-induced MPC [75].

Canonical MPC is dependent on PI3K, which has been shown to be required for macropinosome formation, trafficking and fusion [54, 76] and thus is sensitive to PI3K inhibition. However, it is now clear that distinct types of MPC exist, and different PI3K-dependent and PI3K-independent pathways have been described [77]. For example, different strains of vaccinia virus have been shown to use distinctive PI3K-dependent and independent MPC-like entry routes to infect HeLa cells [57]. Although further studies will be required to confirm our findings, our observation that BTV infection was not inhibited by wortmannin suggest that the entry route used by BTV to infect BFA cells does not require PI3K.

Infection by BTV whole virus particles requires virus exposure to low pH during cell-entry [17, 18] and our experiments confirm that BTV infection of BFA is also dependent on low pH. While macropinosomes remain to be fully characterized, there is good evidence that they undergo a maturation process similar to early-endosomes that involves acidification [78]. In addition, macropinosomes can become acidified by fusion with acidic late-endosomes or endolysosomes [79], which could allow exposure of incoming virus to a low pH environment [80]. Thus, it is highly likely that viruses taken up by MPC or MPC-like pathways will be exposed to a low pH environment during entry.

As outlined in the Introduction, cell-entry is challenging for arboviruses as they need to infect cells from widely diverse vertebrate and invertebrate hosts. Therefore, to achieve cell-entry it is possible that BTV could utilize ubiquitous receptors and entry mechanisms, or enter different cells using diverse receptors and pathways. Indeed early evidence suggested that BTV might be able to exploit more than one entry mechanism, possibly depending on virus serotype and/or the cell type [17, 18]. However, these studies used high-passage tissue-culture virus isolates and cells that were not derived from the natural mammalian hosts and it is possible that cell-entry could have been influenced by virus adaptations that occur during repeated passages in cultured cells (see Introduction). Thus our studies are the first to use a low-passage virulent virus isolate and cells derived from a natural bovine host and suggest that a MPC-like pathway may be a prominent cell-entry route used by BTV to infect endothelial cells. This could have significance *in vivo* as MPC results in the non-specific uptake of membrane receptors and other membrane-associated particles, which could be an advantage for viruses, as they may not need to bind specific receptors for internalization [54]. In many cell types MPC requires activation [76, 81] while in others, such as macrophages and dendritic cells (DC), MPC is constitutively active [82, 83]. With this in mind, a number of studies have concluded that several leucocyte subsets, including macrophages and conventional dendritic cells are likely to be sites of initial virus replication and play a role in BTV dissemination in infected ruminant hosts [22–25, 84]. Thus, the ability to use MPC may be an important determinant of BTV transmission between hosts and the tissue tropism within ruminants.

In conclusion, although we cannot rule out the possibility that other endocytosis pathways are used, our results show that a low-passage insect-cell BTV-1 isolate, that was derived from a virulent BTV strain, most likely utilizes a MPC-like endocytosis pathway as the preferred entry route to infect natural target endothelial cells derived from the bovine hosts. It is interesting to speculate that the ability to use MPC may be an advantage during transmission between invertebrate and vertebrate hosts and thereby facilitate the global success of BTV.

METHODS

Cell lines

KC cells were originally derived from embryonic tissues of *Culicoides sonorensis* [32] and propagated at 28 °C in *Schneiders* insect media (Sigma) with L-glutamine (Sigma) supplemented with 10 % FBS (Sigma), 1 % penicillin/streptomycin (Life Technologies) and 1 % amphotericin B

(Sigma). Bovine Foetal Aorta Endothelial Foetal (BFA) cells were from the European Collection of Cell Cultures (ECACC 87022601) and propagated at 37 °C in F12-Hams media (Sigma), supplemented as above but without amphotericin B.

Virus purification and characterization

BTV-1/KC3 was derived from a virulent 'western' isolate, BTV-1 GIB2007 [The Pirbright Institute (TPI), BTV reference collection BTV-1 GIB2007/01]. This virus was isolated by inoculation of KC cells with infected sheep blood obtained during the BTV-1 outbreak in Gibralter, 2007. The recovered virus (BTV-1 GIB2007/01) was passaged twice more in KC cells before virus purification essentially as described [85], with the exception that infected cells were harvested by manual scraping from culture flasks. Viral titre was determined by fluorescent TCID50 using BFA cells in 96-well tissue culture plates. At 3 days post-infection the cells were fixed using 4 % paraformaldehyde (PFA) (Sigma) for 0.5 h, permeabilized with 0.2 % Triton X-100 (Sigma) in PBS (Gibco) and incubated with anti-BTV-1 polyclonal guinea pig (GP) sera (Orbivirus reference antibody ORAB 279 1 : 2000) in 0.5 % bovine serum albumin (BSA; from Sigma)/PBS for 1 h at room temperature (RT). Following three washes with PBS, a goat anti-GP IgG AlexaFluor-488 secondary antibody (Life Technologies) (1 : 500 in 0.5 %/PBS) was added for 1 h at RT and the cells then washed with PBS. Plates were read to detect fluorescent cells using the ELISpot Reader (AID Elispot). Viral titre ($10^{6.5}TCID_{50}$/ml) was calculated according to previous methodology [86].

Full-length sequencing of individual BTV genome segments was carried out by Sanger sequencing using the BigDye terminator v3.1 kit (Applied Biosystems, Life Technologies, USA) on a 3730 DNA Genetic Analyzer (Applied Biosystems) as previously described [87]. Consensus sequences from each segment were analysed using DNASTAR Lasergene 11 (DNAStar).

Reagents, ligands and pharmacological inhibitors

AlexaFluor-647 labelled transferrin and dextran and AlexaFluor-488-labelled phalloidin were from Life Technologies and CytoPainter Phalloidin-405 from Abcam. Nuclear stains, 4′6-Diamidino-2-Phenylindole (DAPI) and ToPro3 were from Thermo Scientific. PMA (phorbol 12-myristate 13-acetate), Cytochalasin D, Wortmannin, EIPA and cell culture grade DMSO (Dimethylsulphoxide) were supplied by Sigma. Dynasore, dyngo4a, chlorpromazine hydrochloride and pitstop-2 were from Abcam, and IPA3 and ammonium chloride were from Cabiochem and Fluka, respectively. All inhibitors were dissolved in DMSO except for ammonium chloride, which was dissolved in GMEM (Glasgow's minimum essential media) from Sigma, and chlorpromazine hydrochloride, which was dissolved in deionized water. Stock solutions were further diluted in serum-free cell culture media for final concentration given for respective experiments.

Infection conditions, inhibitor studies and cell transfections

BFA cells were infected with purified virus (m.o.i.=<1) in serum-free F12-Hams media (Sigma) for 1 h at 37 °C. The cells were then washed three times with PBS and infection continued in cell culture media but supplemented with 1 % FBS. Cells were pre-treated with pharmacological inhibitors for 0.5 h before infection or the inhibitors were added after infection was initiated as indicated on the figures. After addition, the inhibitor remained present throughout the assay. The control (mock-treated) cells were treated with an equivalent concentration of the appropriate drug diluent. Mammalian expression plasmids for GFP-tagged, WT and dominant-negative (DN) dynamin-2 (Dyn2) splice variant ('aa', 'bb' and 'ba') were supplied by Mark McNiven (Mayo Clinic, Rochester, USA) [53]. Mammalian expression plasmids for GFP-tagged DN eps15 (DIII and EH29) and the control plasmid (D3Δ2) were supplied by Alexandra Benmerah (Universte Paris Descarte, Paris, France). Cell transfections used 1 µg plasmid DNA and XtremeGene 9 (Roche) in a 6 : 1 (reagent/plasmid) ratio as per manufacturers' instructions 16 h prior to infection. Infections were stopped by incubating the cells in 4 % PFA for 1 h on ice. For entry studies infections were stopped as indicated on the figures whereas all other infections were stopped at 12 h p.i.

Flow cytometry experiments

Intracellular labelling of infected cells: Infected (and mock-infected) cells in 4 % PFA were permeabilized with 0.2 % Saponin (Sigma) in 1 % BSA in PBS for 20 min. Viral capsid proteins were labelled using a primary anti-BTV-1, rabbit polyclonal sera (*Orbivirus* reference antibody ORAB 276) at 1 : 4000 in 1 % BSA/0.2 % Saponin/PBS (FACS Buffer) for 1 h and a goat, anti-rabbit IgG AlexaFluor-647 secondary antibody (Life Technologies) (1/500 in FACS Buffer) for 45 min. Following each incubation with antibodies cells were washed three times by 5 min agitation in FACS buffer and subsequent centrifugation at 333 g for 3 min). Following the last wash, pelleted cells were resuspended in 350 µl PBS and transferred to FACS tubes (BD Biosciences) for subsequent analysis. Control ligand uptake: BFA cells were serum starved by incubation in serum-free cell culture media for 45 min changing the media every 15 min and then allowed to take up AlexaFluor-647 transferrin (10 µg ml^{-1})/dextran (0.5 mg ml^{-1}) for 15 min. At the end of uptake, cells were placed on ice and fixed with 4 % paraformaldehyde for 1 h. Cells were then washed in PBS, resuspended in 350 µl PBS and transferred to FACS tubes (BD Biosciences) for subsequent analysis.

Data was collected on the LSR Fortessa (BD Biosciences) using BD FACSDivaTM software and exported as flow cytometry standard (FCS) files and analysed with DeNovo, FCS Express v5 software. Cells were stained with Near IR Live/Dead stain (Life Technologies) using manufacturers' instructions, allowing live and dead cells to be distinguishable by fluorescence staining and gating of viable cells. Cell debris was removed from the analysis by gating cell

populations using forward and side scatter (SSC) and single cell populations in SSC area versus SSC height. For experiments using pharmacological inhibitors the threshold for the detection of infected cells (i.e. virus positive cells) was set using uninfected cells incubated with the primary and secondary antibodies. Infection levels of drug-treated cells were normalised to infection of mock-treated control cells. For transfection experiments using GFP-tagged proteins, the level of infection of the GFP positive population for DN expressing cells was normalized to infection of the GFP positive populations expressing the matched WT or control construct. Mean fluorescent intensity (M.F.I.) was used to quantify uptake of control ligands. The background threshold was set by using cells that were exposed to ligand at 4 °C.

Immunofluorescence confocal microscopy

Experiments were carried out using cells on glass coverslips (VWR). For entry experiments, cells were incubated with purified virus (m.o.i.=10) in serum-free media on ice for 1 h to allow virus adsorption and entry synchronization. After adsorption, the cells were washed three times with serum-free cell-culture media and warmed to 37 °C for 0.5, 1 or 1.5 or 2 h p.i. (as indicated on the figures) and then fixed and processed for microscopy labelling for BTV capsid proteins as follows. The cells were placed on ice and fixed with 4 % PFA for 1 h and then immersed in PBS. Cells were permeabilized using 0.2 % saponin in PBS for 20 min and then blocked using 10% Normal Goat Serum (Harlan Lab Sera) and 1 % Teleostean Gelatin (Sigma) in TBS (block buffer) for 0.5 h. Viral capsid proteins were detected using ORAB 276 (1 : 1000) and a goat anti-rabbit IgG AlexaFluor-568 secondary antibody (Life Technologies) (1/200) in block buffer. The cells were incubated sequentially for 1 h each with the primary antibody and secondary antibodies, with 3×5 min PBS washes between antibody incubations. For transferrin uptake, BFA cells were incubated in serum-free cell-culture media for 45 min changing the media every 15 min and then allowed to take up AlexaFluor-568 transferrin (10 μg ml^{-1}) for 15 min at 37C. At the end of uptake, cells were placed on ice and fixed with 4 % paraformaldehyde for 1 h. Cell nuclei were stained with 4′,6-Diamidino-2-Phenylindole (DAPI) or TO-PRO-3 and coverslips mounted in Vectashield mounting medium for fluorescence (VectorLabs). The actin cortex was labelled using (1/20) AlexaFluor-488-labelled phalloidin (Life technologies) in PBS for 20 min or CytoPainter-405 Phalloidin as per manufacturers' instructions. Cells were viewed using the Leica TCS SP8 Confocal laser-scanning microscope and optical sections recorded using either the 63 or 40x oil-immersion objective with a numerical aperture of 1.4 and 1.25, respectively. The data are shown as single optical sections through the middle of the cell. All data were collected sequentially to minimize bleed-through fluorescent signals. Images were processed using Adobe Photoshop software.

Cytotoxicity assays

BFA cells were seeded onto optically clear bottom, white-sided plates (Perkin Elmer) the day before the assay. When cells were 80 % confluent, cells were treated with a range of concentrations of the pharmacological inhibitors for 12.5 h. Cell viability was determined using the CellTiter-Glo luminescence assay (Promega) as per manufacturers' instructions using Hidex chameleon luminometer.

Statistical analysis

All experiments were carried out using triplicate samples for at least two independent experiments. Data from repeated experiments were combined prior to statistical analysis. The statistical significance of results of comparisons between experimental groups were determined by one-way ANOVA with Tukey's correction, which was carried out using Minitabv17.

Funding information
For this project L.S. was funded by a BBSRC/The Pirbright Institute (TPI) studentship (BB/F016492/1). This work was also supported by the BBSRC initiative grant (BB/L014203/1), T.J. by BBSRC grant (BBS/E/I/00001716) and K.D. by BBSRC projects BBS/E/I/00001728 and BBS/E/I/00007034. K.N. was supported by Wellcome Trust grant (092806/Z/10/Z). L.C. was funded by BBSRC/TPI studentship (BBS/E/I/00001860).

Acknowledgements
We would like to thank the Biotechnology and Biological Sciences Research Council (BBSRC) for funding this project. We are grateful to Alexandra Benmerah for supplying the DN and control eps15 constructs and Mark McNiven for supplying the WT and DN dynamin-2 splice variant constructs.

Conflicts of interest
The authors declare that there are no conflicts of interest.

References

1. **Kilpatrick AM, Randolph SE.** Drivers, dynamics, and control of emerging vector-borne zoonotic diseases. *Lancet* 2012;380:1946–1955.
2. **Kuno G, Chang GJ.** Biological transmission of arboviruses: reexamination of and new insights into components, mechanisms, and unique traits as well as their evolutionary trends. *Clin Microbiol Rev* 2005;18:608–637.
3. **Maan S, Maan NS, Belaganahalli MN, Potgieter AC, Kumar V *et al.*** Development and evaluation of real time RT-PCR assays for detection and typing of bluetongue virus. *PLoS One* 2016;11:e0163014.
4. **Lorusso A, Sghaier S, di Domenico M, Barbria ME, Zaccaria G *et al.*** Analysis of bluetongue serotype 3 spread in Tunisia and discovery of a novel strain related to the bluetongue virus isolated from a commercial sheep pox vaccine. *Infect Genet Evol* 2018;59:63–71.
5. **Marcacci M, Sant S, Mangone I, Goria M, Dondo A *et al.*** One after the other: a novel bluetongue virus strain related to Toggenburg virus detected in the Piedmont region (North-western Italy), extends the panel of novel atypical BTV strains. *Transbound Emerg Dis* 2018;65:370–374.
6. **Sun EC, Huang LP, Xu QY, Wang HX, Xue XM *et al.*** Emergence of a novel bluetongue virus serotype, China 2014. *Transbound Emerg Dis* 2016;63:585–589.
7. **Savini G, Puggioni G, Meloni G, Marcacci M, di Domenico M *et al.*** Novel putative bluetongue virus in healthy goats from Sardinia, Italy. *Infect Genet Evol* 2017;51:108–117.

8. Carpenter S, Wilson A, Mellor PS. Culicoides and the emergence of bluetongue virus in northern Europe. *Trends Microbiol* 2009;17: 172–178.
9. Samy AM, Peterson AT. Climate change influences on the global potential distribution of bluetongue virus. *PLoS One* 2016;11: e0150489.
10. Verwoerd DW, Louw H, Oellermann RA. Characterization of bluetongue virus ribonucleic acid. *J Virol* 1970;5:1–7.
11. Grimes JM, Burroughs JN, Gouet P, Diprose JM, Malby R *et al.* The atomic structure of the bluetongue virus core. *Nature* 1998; 395:470–478.
12. Huismans H, Erasmus BJ. Identification of the serotype-specific and group-specific antigens of bluetongue virus. *Onderstepoort J Vet Res* 1981;48:51–58.
13. Zhang X, Boyce M, Bhattacharya B, Zhang X, Schein S *et al.* Bluetongue virus coat protein VP2 contains sialic acid-binding domains, and VP5 resembles enveloped virus fusion proteins. *Proc Natl Acad Sci USA* 2010;107:6292–6297.
14. Eaton BT, Crameri GS. The site of bluetongue virus attachment to glycophorins from a number of animal erythrocytes. *J Gen Virol* 1989;70:3347–3353.
15. Hassan SS, Roy P. Expression and functional characterization of bluetongue virus VP2 protein: role in cell entry. *J Virol* 1999;73: 9832–9842.
16. Eaton BT, Hyatt AD, Brookes SM. The replication of bluetongue virus. *Curr Top Microbiol Immunol* 1990;162:89–118.
17. Forzan M, Marsh M, Roy P. Bluetongue virus entry into cells. *J Virol* 2007;81:4819–4827.
18. Gold S, Monaghan P, Mertens P, Jackson T. A clathrin independent macropinocytosis-like entry mechanism used by bluetongue virus-1 during infection of BHK cells. *PLoS One* 2010;5:e11360.
19. Mercer J, Schelhaas M, Helenius A. Virus entry by endocytosis. *Annu Rev Biochem* 2010;79:803–833.
20. Schmid SL, Frolov VA. Dynamin: functional design of a membrane fission catalyst. *Annu Rev Cell Dev Biol* 2011;27:79–105.
21. Henley JR, Krueger EW, Oswald BJ, McNiven MA. Dynamin-mediated internalization of caveolae. *J Cell Biol* 1998;141:85–99.
22. Stott JL, Blanchard-Channell M, Scibienski RJ, Stott ML. Interaction of bluetongue virus with bovine lymphocytes. *J Gen Virol* 1990;71:363–368.
23. Hemati B, Contreras V, Urien C, Bonneau M, Takamatsu HH *et al.* Bluetongue virus targets conventional dendritic cells in skin lymph. *J Virol* 2009;83:8789–8799.
24. Ruscanu S, Pascale F, Bourge M, Hemati B, Elhmouzi-Younes J *et al.* The double-stranded RNA bluetongue virus induces type I interferon in plasmacytoid dendritic cells via a MYD88-dependent TLR7/8-independent signaling pathway. *J Virol* 2012;86:5817–5828.
25. Darpel KE, Monaghan P, Simpson J, Anthony SJ, Veronesi E *et al.* Involvement of the skin during bluetongue virus infection and replication in the ruminant host. *Vet Res* 2012;43:40.
26. MacLachlan NJ, Drew CP, Darpel KE, Worwa G. The pathology and pathogenesis of bluetongue. *J Comp Pathol* 2009;141:1–16.
27. Melzi E, Caporale M, Rocchi M, Martín V, Gamino V *et al.* Follicular dendritic cell disruption as a novel mechanism of virus-induced immunosuppression. *Proc Natl Acad Sci USA* 2016;113:E6238–E6247.
28. Demaula CD, Leutenegger CM, Bonneau KR, MacLachlan NJ. The role of endothelial cell-derived inflammatory and vasoactive mediators in the pathogenesis of bluetongue. *Virology* 2002;296:330–337.
29. O'Donnell V, Larocco M, Baxt B. Heparan sulfate-binding foot-and-mouth disease virus enters cells via caveola-mediated endocytosis. *J Virol* 2008;82:9075–9085.
30. Su CM, Liao CL, Lee YL, Lin YL. Highly sulfated forms of heparin sulfate are involved in japanese encephalitis virus infection. *Virology* 2001;286:206–215.
31. Janowicz A, Caporale M, Shaw A, Gulletta S, di Gialleonardo L *et al.* Multiple genome segments determine virulence of bluetongue virus serotype 8. *J Virol* 2015;89:5238–5249.
32. Wechsler SJ, McHolland LE, Tabachnick WJ. Cell lines from Culicoides variipennis (Diptera: Ceratopogonidae) support replication of bluetongue virus. *J Invertebr Pathol* 1989;54:385–393.
33. Moulin V, Noordegraaf CV, Makoschey B, van der Sluijs M, Veronesi E *et al.* Clinical disease in sheep caused by bluetongue virus serotype 8, and prevention by an inactivated vaccine. *Vaccine* 2012;30:2228–2235.
34. McCluskey A, Daniel JA, Hadzic G, Chau N, Clayton EL *et al.* Building a better dynasore: the dyngo compounds potently inhibit dynamin and endocytosis. *Traffic* 2013;14:1272–1289.
35. Cao H, Garcia F, McNiven MA. Differential distribution of dynamin isoforms in mammalian cells. *Mol Biol Cell* 1998;9:2595–2609.
36. Cao H, Chen J, Awoniyi M, Henley JR, McNiven MA. Dynamin 2 mediates fluid-phase micropinocytosis in epithelial cells. *J Cell Sci* 2007;120:4167–4177.
37. Hanover JA, Willingham MC, Pastan I. Kinetics of transit of transferrin and epidermal growth factor through clathrin-coated membranes. *Cell* 1984;39:283–293.
38. Wang LH, Rothberg KG, Anderson RG. Mis-assembly of clathrin lattices on endosomes reveals a regulatory switch for coated pit formation. *J Cell Biol* 1993;123:1107–1117.
39. von Kleist L, Stahlschmidt W, Bulut H, Gromova K, Puchkov D *et al.* Role of the clathrin terminal domain in regulating coated pit dynamics revealed by small molecule inhibition. *Cell* 2011;146: 471–484.
40. Benmerah A, Bayrou M, Cerf-Bensussan N, Dautry-Varsat A. Inhibition of clathrin-coated pit assembly by an Eps15 mutant. *J Cell Sci* 1999;112:1303–1311.
41. Benmerah A, Lamaze C, Bègue B, Schmid SL, Dautry-Varsat A *et al.* AP-2/Eps15 interaction is required for receptor-mediated endocytosis. *J Cell Biol* 1998;140:1055–1062.
42. Ehrlich M, Boll W, van Oijen A, Hariharan R, Chandran K *et al.* Endocytosis by random initiation and stabilization of clathrin-coated pits. *Cell* 2004;118:591–605.
43. Doyon JB, Zeitler B, Cheng J, Cheng AT, Cherone JM *et al.* Rapid and efficient clathrin-mediated endocytosis revealed in genome-edited mammalian cells. *Nat Cell Biol* 2011;13:331–337.
44. Mercer J, Helenius A. Virus entry by macropinocytosis. *Nat Cell Biol* 2009;11:510–520.
45. Greber UF. Signalling in viral entry. *Cell Mol Life Sci* 2002;59:608–626.
46. Kerr MC, Teasdale RD. Defining Macropinocytosis. *Traffic* 2009;10: 364–371.
47. Hoffmann PR, Decathelineau AM, Ogden CA, Leverrier Y, Bratton DL *et al.* Phosphatidylserine (PS) induces PS receptor-mediated macropinocytosis and promotes clearance of apoptotic cells. *J Cell Biol* 2001;155:649–660.
48. Cruz-Oliveira C, Freire JM, Conceição TM, Higa LM, Castanho MA *et al.* Receptors and routes of dengue virus entry into the host cells. *FEMS Microbiol Rev* 2015;39:155–170.
49. Conner SD, Schmid SL. Regulated portals of entry into the cell. *Nature* 2003;422:37–44.
50. Li L, Wan T, Wan M, Liu B, Cheng R *et al.* The effect of the size of fluorescent dextran on its endocytic pathway. *Cell Biol Int* 2015;39: 531–539.
51. Harris C, Fliegel L. Amiloride and the Na(+)/H(+) exchanger protein: mechanism and significance of inhibition of the Na(+)/H(+) exchanger (review). *Int J Mol Med* 1999;3:315–321.
52. Dharmawardhane S, Schürmann A, Sells MA, Chernoff J, Schmid SL *et al.* Regulation of macropinocytosis by p21-activated kinase-1. *Mol Biol Cell* 2000;11:3341–3352.

53. Deacon SW, Beeser A, Fukui JA, Rennefahrt UE, Myers C *et al.* An isoform-selective, small-molecule inhibitor targets the autoregulatory mechanism of p21-activated kinase. *Chem Biol* 2008;15: 322–331.
54. Mercer J, Helenius A. Gulping rather than sipping: macropinocytosis as a way of virus entry. *Curr Opin Microbiol* 2012;15:490–499.
55. Posor Y, Eichhorn-Gruenig M, Puchkov D, Schöneberg J, Ullrich A *et al.* Spatiotemporal control of endocytosis by phosphatidylinositol-3,4-bisphosphate. *Nature* 2013;499:233–237.
56. Lindmo K, Stenmark H. Regulation of membrane traffic by phosphoinositide 3-kinases. *J Cell Sci* 2006;119:605–614.
57. Mercer J, Knébel S, Schmidt FI, Crouse J, Burkard C *et al.* Vaccinia virus strains use distinct forms of macropinocytosis for host-cell entry. *Proc Natl Acad Sci USA* 2010;107:9346–9351.
58. de Vries E, Tscherne DM, Wienholts MJ, Cobos-Jiménez V, Scholte F *et al.* Dissection of the influenza A virus endocytic routes reveals macropinocytosis as an alternative entry pathway. *PLoS Pathog* 2011;7:e1001329.
59. Hetzenecker S, Helenius A, Krzyzaniak MA. HCMV induces macropinocytosis for host cell entry in fibroblasts. *Traffic* 2016;17:351–368.
60. Krzyzaniak MA, Zumstein MT, Gerez JA, Picotti P, Helenius A. Host cell entry of respiratory syncytial virus involves macropinocytosis followed by proteolytic activation of the F protein. *PLoS Pathog* 2013;9:e1003309.
61. Gonçalves-Carneiro D, McKeating JA, Bailey D. The measles virus receptor SLAMF1 can mediate particle endocytosis. *J Virol* 2017; 91.
62. Mertens PP, Burroughs JN, Walton A, Wellby MP, Fu H *et al.* Enhanced infectivity of modified bluetongue virus particles for two insect cell lines and for two Culicoides vector species. *Virology* 1996;217:582–593.
63. Wadia JS, Stan RV, Dowdy SF. Transducible TAT-HA fusogenic peptide enhances escape of TAT-fusion proteins after lipid raft macropinocytosis. *Nat Med* 2004;10:310–315.
64. Ivanov AI, Nusrat A, Parkos CA. Endocytosis of epithelial apical junctional proteins by a clathrin-mediated pathway into a unique storage compartment. *Mol Biol Cell* 2004;15:176–188.
65. Fretz M, Jin J, Conibere R, Penning NA, Al-Taei S *et al.* Effects of Na+/H+ exchanger inhibitors on subcellular localisation of endocytic organelles and intracellular dynamics of protein transduction domains HIV-TAT peptide and octaarginine. *J Control Release* 2006;116:247–254.
66. Lagana A, Vadnais J, Le PU, Nguyen TN, Laprade R *et al.* Regulation of the formation of tumor cell pseudopodia by the Na(+)/H(+) exchanger NHE1. *J Cell Sci* 2000;113:3649–3662.
67. Meier O, Boucke K, Hammer SV, Keller S, Stidwill RP *et al.* Adenovirus triggers macropinocytosis and endosomal leakage together with its clathrin-mediated uptake. *J Cell Biol* 2002;158: 1119–1131.
68. Roth MG. Integrating actin assembly and endocytosis. *Dev Cell* 2007;13:3–4.
69. Sandvig K, Kavaliauskiene S, Skotland T. Clathrin-independent endocytosis: an increasing degree of complexity. *Histochem Cell Biol* 2018;150:107–118.
70. Ferguson SM, de Camilli P. Dynamin, a membrane-remodelling GTPase. *Nat Rev Mol Cell Biol* 2012;13:75–88.
71. Carter GC, Bernstone L, Baskaran D, James W. HIV-1 infects macrophages by exploiting an endocytic route dependent on dynamin, Rac1 and Pak1. *Virology* 2011;409:234–250.
72. Buccione R, Orth JD, McNiven MA. Foot and mouth: podosomes, invadopodia and circular dorsal ruffles. *Nat Rev Mol Cell Biol* 2004; 5:647–657.
73. Khan AG, Pickl-Herk A, Gajdzik L, Marlovits TC, Fuchs R *et al.* Entry of a heparan sulphate-binding HRV8 variant strictly depends on dynamin but not on clathrin, caveolin, and flotillin. *Virology* 2011;412:55–67.
74. Liu YW, Surka MC, Schroeter T, Lukiyanchuk V, Schmid SL. Isoform and splice-variant specific functions of dynamin-2 revealed by analysis of conditional knock-out cells. *Mol Biol Cell* 2008;19: 5347–5359.
75. Schlunck G, Damke H, Kiosses WB, Rusk N, Symons MH *et al.* Modulation of Rac localization and function by dynamin. *Mol Biol Cell* 2004;15:256–267.
76. Yoshida S, Hoppe AD, Araki N, Swanson JA. Sequential signaling in plasma-membrane domains during macropinosome formation in macrophages. *J Cell Sci* 2009;122:3250–3261.
77. Jiang J, Kolpak AL, Bao ZZ. Myosin IIB isoform plays an essential role in the formation of two distinct types of macropinosomes. *Cytoskeleton* 2010;67:32–42.
78. Rizopoulos Z, Balistreri G, Kilcher S, Martin CK, Syedbasha M *et al.* Vaccinia virus infection requires maturation of macropinosomes. *Traffic* 2015;16:814–831.
79. Racoosin EL, Swanson JA. Macropinosome maturation and fusion with tubular lysosomes in macrophages. *J Cell Biol* 1993;121: 1011–1020.
80. Saeed MF, Kolokoltsov AA, Albrecht T, Davey RA. Cellular entry of ebola virus involves uptake by a macropinocytosis-like mechanism and subsequent trafficking through early and late endosomes. *PLoS Pathog* 2010;6:e1001110.
81. Welliver TP, Swanson JA. A growth factor signaling cascade confined to circular ruffles in macrophages. *Biol Open* 2012;1:754–760.
82. Sallusto F, Cella M, Danieli C, Lanzavecchia A. Dendritic cells use macropinocytosis and the mannose receptor to concentrate macromolecules in the major histocompatibility complex class II compartment: downregulation by cytokines and bacterial products. *J Exp Med* 1995;182:389–400.
83. Canton J, Schlam D, Breuer C, Gütschow M, Glogauer M *et al.* Calcium-sensing receptors signal constitutive macropinocytosis and facilitate the uptake of NOD2 ligands in macrophages. *Nat Commun* 2016;7:11284.
84. Barratt-Boyes SM, Rossitto PV, Stott JL, MacLachlan NJ. Flow cytometric analysis of in vitro bluetongue virus infection of bovine blood mononuclear cells. *J Gen Virol* 1992;73:1953–1960.
85. Mertens PP, Burroughs JN, Anderson J. Purification and properties of virus particles, infectious subviral particles, and cores of bluetongue virus serotypes 1 and 4. *Virology* 1987;157:375–386.
86. Karber. [Not Available]. Hygienische Schäden infolge falscher oder mangelhafter Ernährung. *Zentralbl Bakteriol Orig* 1949;153: 36–43.
87. Maan S, Rao S, Maan NS, Anthony SJ, Attoui H *et al.* Rapid cDNA synthesis and sequencing techniques for the genetic study of bluetongue and other dsRNA viruses. *J Virol Methods* 2007;143: 132–139.